On the double-band luminescence of ZnO nanoparticles

Lijie Li[1]

[1] *Multidisciplinary Nanotechnology Centre, College of Engineering, Swansea University, Bay Campus, SA1 8EN, Swansea, UK*

PACS 78.20.Bh – Theory, models, and numerical simulation
PACS 78.45.+h – Stimulated emission
PACS 78.55.-m – Photoluminescence, properties and materials

Abstract –Two luminescence bands from zinc oxide (ZnO) nanoparticles have been known and experimentally observed previously. The unanswered question is the mechanism leading to the visible spectrum in the blue or green region. So far there have been many postulations trying to elucidate this phenomenon, but none of them gives a mathematical expression that simultaneously expresses these two spectra. Here we interpret this phenomenon as the combination of distribution functions and the density of states of electrons and holes, precisely the product of the both. From the analysis, the narrow UV emission is predominantly attributed to the quantum confinement, and the product of the density of states and the distribution functions determines the visible spectrum. We find that varying the density and the effective mass of holes causes pronounced effect on both UV and visible, which reflects the fact of acceptors taking the main responsibility in the experimental observations.

Introduction. – Wide visible luminescence band of ZnO nanoparticles have attracted vast interests due to its potential applications in optoelectronics and sensors. Although the narrow UV band emission of ZnO has been firmly attributed to the excitonic emission, the visible emission is until now still open to debate. The explanations to the visible emission are mainly described as the effect caused by additional acceptors [1], such as copper (structured and structureless) [2] [3], oxygen vacancies [4] [5] [6], Indium doping [7] [8], zinc implantation [9], additional nitrogen acceptors by thermal annealing [10] [11], yttrium doping [12], Lithium acceptor [13], and Aluminium doping [14]. All of above can be summarised to the imperative role played by the acceptors. Most recent research on this subject reinforce or confirm previous argument [12, 15–20]. So far descriptive explanations have been provided on the various mechanisms making ZnO exhibit visible luminescence. Many controversial statements are surrounding the arguments of electron transiting from various vacancies to the valence band [21] [22], or from conduction band to their interstitials [23]. However these arguments are not well supported by the continuous and stable visible emission as electrons trapped in the vacancies or defects can vary. Also the vacancies and defects are very uncontrollable and unpredictable, which find hard to explain the stable visible spectrum. Of these observed visible bands, green emission sparks several elucidations, such as it may be caused by electron transiting from vacancy to the valence band [24] or may be due to electron transition from conduction band to vacancy [25]. There have been longer wavelength emissions such as orange and red emission [26] [27]. Figure 1 shows the previously reported observation of double band emissions from ZnO nanoparticles [28], and a scanning electron microscope image of ZnO nanowires [29]. In this work we propose a theory that can predict the UV and visible emissions simultaneously. It reveals that the visible emission is the combined effect of the distribution functions and density of states of electrons and holes. Effective masses, density of electrons/holes and the temperature have been investigated to show their effect to the luminescence.

Analysis and Results. – Luminescence comes from electrons transiting from higher energy states in the conduction band to lower energy states in the valance band. In a nutshell, the bandgap of the material directly determines the luminescence spectrum. For the nanometre sized ZnO structures, quantum confinement increases the bulk bandgap E_g by $E_{e,h} = \frac{\hbar^2\pi^2}{2m_{e,h}r^2}$, where $\hbar$ is the reduced Planck's constant, and $m_{e,h}$ denote the effective

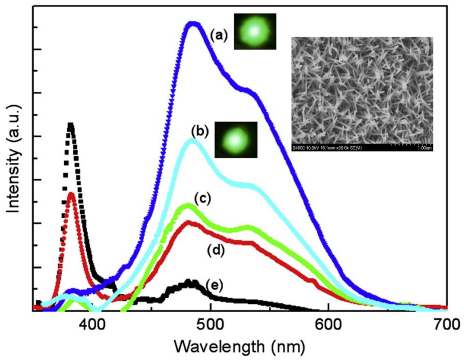

Fig. 1: Experimental observation of double-band luminescence of ZnO nanoparticles (Reprinted from [28] with permission from Elsevier). Inserted graph is a scanning electron microscopic image of ZnO nanowires (Reprinted from [29] with permission from Elsevier).

masses of electrons and holes. r is the radius of the nanoparticle. In the analysis only ground states are taken into account. Exciton binding energy decreases the E_g by $E_{ex} = \frac{m_r e^4}{32\pi^2\hbar^2\epsilon_r^2\epsilon_0^2} = \frac{e^2}{8\pi\epsilon_r\epsilon_0\alpha_0^*}$, where $\alpha_0^* = \frac{4\pi\epsilon_r\epsilon_0\hbar^2}{e^2 m_r}$ stands for the exciton Bohr radius [30]. Relative dielectric constant and permittivity in free space are represented by ϵ_r and ϵ_0. Here $m_r = m_e m_h/(m_e + m_h)$ is the reduced mass for the electrons and holes characterizing macroscopically conductivity. Therefore the effective bandgap E_n after considering all these effects for the nanoparticles is expressed by

$$E_n = Eg + E_e + E_h - E_{ex} \tag{1}$$

This is the energy that an electron losses through transiting from the ground state of the conduction band to the ground state of the valence band, subsequently generating a photon with energy $\hbar\omega$, where ω is the frequency of the photon. The above is the basics of the luminescence of the semiconductor nanoparticles, and this well explains the UV luminescence. Taking all essential parameters, the calculated maximum is at 372 nm. In order to obtain more detailed results, factors such as the number of electrons in higher energy states and the number of holes in the lower energy states available for taking part in the recombination process, as well as the number of excitation energy from the incident photons, i.e. number of photons will be required. In the analysis it is assumed that the number of incident photons at all wavelengths are the same. According to the quantum optics theory [31], the emission rate that is the function of the numbers incident photons and numbers free electrons and holes can be expressed as

$$\mathcal{R} = |M_{f,i}|\rho_{op}\mathcal{B}_{op}\rho_e f_c(1 - f_v) \tag{2}$$

Where $|M_{f,i}| \sim |\langle f|\hat{V}|i\rangle|$ represents the interband matrix element of the perturbation $\hat{V}$, for most of semiconductor materials, this matrix does not vary very much, which can be considered as a constant in the calculation. ρ_{op} and $\mathcal{B}_{OP} = (\exp(\frac{\hbar\omega}{k_B T}) - 1)^{-1}$ denote the density of states and Bose-Einstein distribution for the incident photons respectively. As the assumption of constant incident photons number is taken, $\rho_{op}\mathcal{B}_{op}$ remains unchanged. ρ_e, f_c, f_v are density of states for the carriers and Fermi Dirac distributions for electrons in the conduction band and the valence band respectively, $f_{c,v} = (\exp(\frac{E-\mu_{c,v}}{k_B T}) + 1)^{-1}$. Here we use the self-consistent iteration method to derive the chemical potentials $\mu_{c,v}$ ascribed to electrons in the conduction band and holes in the valence band. The density of states for 0D confined nanoparticles can be expressed using a Lorentzian, which is

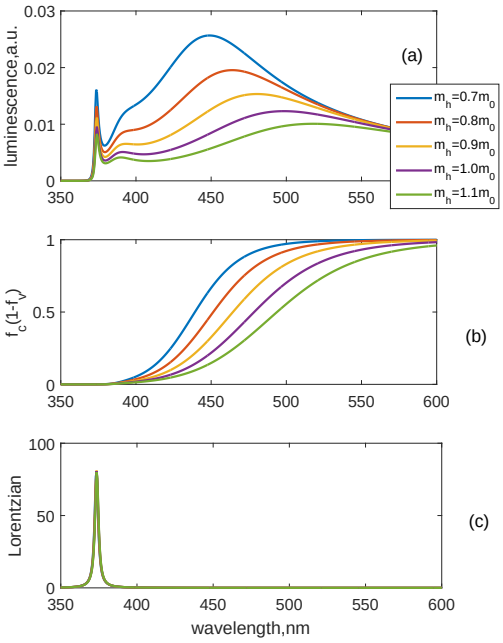

Fig. 2: Calculated luminescence of ZnO nanoparticles due to the factor of the varied hole effective mass m_h. Electron effective mass is taken as $0.23m_0$, and the density of electron-holes pairs remains as $8 \times 10^{22}\ m^{-3}$. (a) Luminescence vs. wavelength. (b) $f_c(1 - f_v)$ vs. wavelength. (c) Lorentzian vs. wavelength.

$$\rho_e(E) = \frac{2}{\pi}\frac{(\hbar/2\tau)}{(E - E_n)^2 + (\hbar/2\tau)^2} \tag{3}$$

Where the $\hbar/\tau$ is the width at half its maximum of the Lorentzian, which is determined by the coupling between the nanoparticle and the outside metal. Empirical value has to be extracted from the experiment, here a value of 25 meV is used. It is envisaged that the emission rate is proportional to the product of a Lorentzian and distribution functions. Therefore it should be expected that an emission spectrum with the peak at the energy of E_n corresponding to the wavelength of around 373 nm in the ultraviolet (UV) region, which has been experimentally observed previously in many literatures. It is the emission

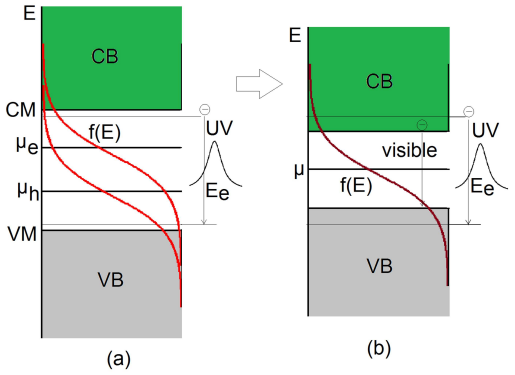

Fig. 3: Schematic graph of the band structure explaining the double-emission of ZnO nanoparticles.

at the visible band that is ambiguous. The parameters and constants used in the simulation are described in the **Appendix**.

In the analysis, we tune the following parameters to observe the phenomena of the luminescence, they are effective mass of the heavy hole, unbalanced numbers of electrons and holes (extra electrons and extra holes), and the temperature.

Effective masses of electrons and holes are virtual values derived from the k-p method for the aim of understanding the energy curves (electrons and holes) in the k-space. Physically it can be interpreted as the mobility of carriers. Large effective mass implies that the carrier is heavy and less mobile, semi-classically explained by the Newton law. Mathematically effective mass can be written as $\frac{1}{m_{e,h}} = \frac{1}{\hbar^2}\frac{d^2E}{dk^2}$. Some materials have larger electron effective mass and some have larger hole effective mass. For ZnO, electron effective mass is smaller than hole's. More to mention that the electron effective mass varies much less than the hole's. Valence band usually contains three sub-bands corresponding to three values of hole effective masses, namely light hole, heavy hole, and split-off. ZnO exhibits direct bandgap, which means that the conduction band minimum is aligned with the valence band maximum. As to three valence bands, light hole and heavy hole share the maximum point when $k = 0$, also known as the Γ point. Split-off band has a ΔE shift form the maximum of the light and heavy hole bands. The light hole energy curve is steeper than that of heavy holes. We shall focus on the heavy hole, as the heavy hole dominates the property of the valence band. This is because the heavy hole curve is much flatter than the light hole, indicating that for a fixed Δk, the density of states of heavy holes is much larger.

Calculation results in **Figure 2** show that there are two spectra with one in the UV, and the other in the visible region. UV emission originated from the Lorentzian depends on the E_n. According to the equation (2). the distribution functions have several determining factors, which are effective mass, carrier concentration, and the temperature.

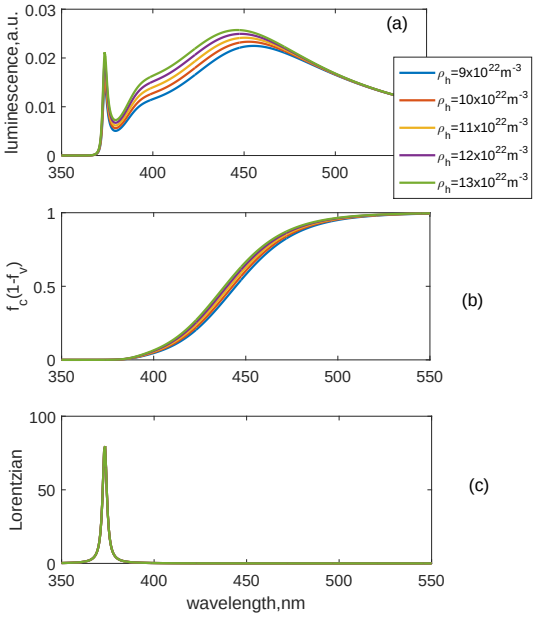

Fig. 4: Results for varying the density of holes. Other parameters are the same as used in Figure 2. The hole effective mass is designated as $0.7m_0$. (a) Luminescence vs. wavelength. (b) $f_c(1-f_v)$ vs. wavelength. (c) Lorentzian vs. wavelength.

We vary the effective mass of the heavy hole from $0.7m_0$ to $1.1m_0$ while keeping other parameters unchanged. It is seen that as the m_h increases, the peak of the visible band shifts to the green region and the amplitude of emission reduces. The UV spectrum does not change except for the reduction of the amplitude. The shift of the visible spectrum is seen due to the flattening of the Fermi function (shown in **Figure 2b**). The appearance of the visible spectrum can be seen as the narrowed bandgap caused by the Fermi level split to one closer to the conduction band (μ_e) and the other closer to the valence band (μ_h) shown in **Figure 3**. The level splitting is due to the increased electron-hole pairs by the incident photons. It is envisaged that when there are excessive electrons and holes, the material becomes highly conductive, in which case the μ_e is very close to the conduction band minimum and the μ_h is very close to the valence band maximum, resembling properties of metals, in which case the visible luminescence arises from the recombination of conduction band electrons below the Fermi energy with holes in the d band [32].

When the density of holes exceeds the density of electrons, luminescence varies as shown in calculated results in **Figure 4**, where the amplitudes of both the band-edge and visible emissions increase when increasing the value from $9 \times 10^{22} m^{-3}$ to $13 \times 10^{22} m^{-3}$. This is understood as the increasing recombination probabilities for the larger number of holes. Compared with the results in **Figure 5**, in which case only the density of electrons increases while

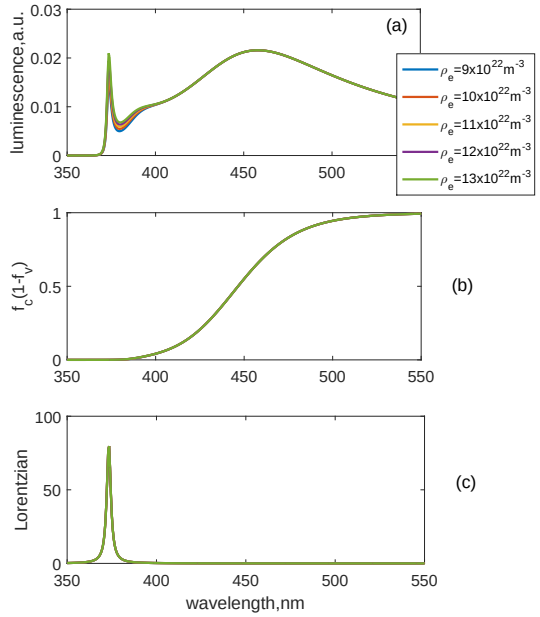

Fig. 5: Model for different values of densities of electrons, density of holes and other parameters remain the same as in Figure 4. (a) Luminescence vs. wavelength. (b) $f_c(1-f_v)$ vs. wavelength. (c) Lorentzian vs. wavelength.

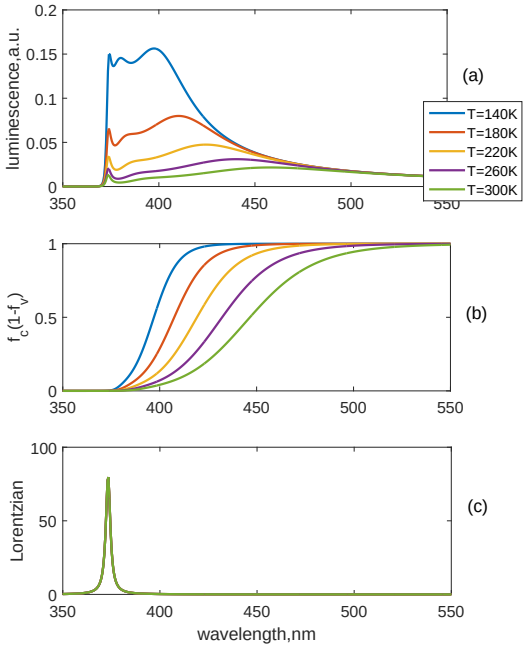

Fig. 6: Simulation of the luminescence from the temperature impact. Temperature changes from 140 K to room temperature. (a) Luminescence vs. wavelength. (b) $f_c(1-f_v)$ vs. wavelength. (c) Lorentzian vs. wavelength.

keeping the density of holes unchanged, which does not affect the visible spectrum. This is seen that increasing the number of electrons does not change the Fermi distributions (**Figure 5b**) at the observable scale.

The temperature has a significant effect on the luminescence, shown in the **Figure 6**. It is demonstrated that when temperature decreases, the visible spectrum shifts to the UV region and joins with the band-edge emission, the emission amplitude is also much increased. This is due to sharpening of the Fermi distribution functions, so that the chemical potential splitting does not cause effective narrowing of bandgap. The emission is dominated by the E_n at very low temperatures.

Conclusion. – To conclude, an elucidation of how the two emission bands appear for ZnO nanoparticles has been described underpinned by the quantum optics theory. It is revealed that this well experimented phenomenon is the effect from the product of distribution functions and quantum confined density of states. The analysis provides a first general equation to simulate these two luminescence spectra simultaneously. Theoretical results matches with previously reported argument, which is the acceptors contributing to the visible luminescence. The work shows that the properties of holes (effective mass and density) have significant impact to the visible luminescence. It opens another view to describe the multi-band luminescence of the ZnO nanoparticles besides ambiguous explanations on the basis of defects and impurities.

Appendix. – In the analysis, constants were taken values as follows: Planck's constant $\hbar = 1.054 \times 10^{-34}$ Js, Boltzmann constant $k_B = 8.617 \times 10^{-5}$ eVK^{-1}, single electron mass $m_0 = 9.109 \times 10^{-31}$ Kg, single electron charge $e = 1.602 \times 10^{-19}$ C, and permittivity of free space $\epsilon_0 = 8.85 \times 10^{-12}$ Fm^{-1}. The relative dielectric constant has been taken as $\epsilon_r = 8.91$ [33], and radius of the nanoparticle was given as 50 nm. The bulk energy bandgap for ZnO was taken as 3.35 eV. The chemical in the Fermi distribution has to be arrived from the density of carriers. For calculating the chemical potential, the carrier density equation is used

$$n = \frac{1}{2\pi^2}\left(\frac{2m_{e,h}}{\hbar^2}\right)^{3/2}\int_0^\infty \frac{E^{1/2}}{\exp(\frac{E-\mu}{k_BT})+1}dE \qquad (4)$$

where an initial μ was given to arrive at n, then iterating the process by increasing/decreasing the μ until n was very close to the pre-set value.

In order to investigate the impact due to the effective mass, effective masses of electrons and holes were initially given as $0.23m_0$ and $0.7m_0$ respectively, then the hole effective mass has been increased from $0.7m_0$ to 1.1 m_0 when keeping electron effective mass unchanged as $0.23m_0$. Equation (2) was used to calculate the emission rate. The results are shown in the Figure 2.

For researching the carriers concentration effect on the luminescence, the densities of electrons and holes were set initially to $8 \times 10^{22}m^{-3}$, then varying each of them from $9 \times 10^{22}m^{-3}$ to $13 \times 10^{22}m^{-3}$. In the temperature

analysis, densities of electrons and holes were all given as $8 \times 10^{22} m^{-3}$, and effective masses of electrons and holes were designated as $0.23m_0$ and $0.7m_0$ respectively.

Acknowledgements. – LL appreciates the support of college of engineering, Swansea University.

REFERENCES

[1] McCluskey M. D., Corolewski C. D., Lv J., Tarun M. C., Teklemichael S. T., Walter E. D., Norton M. G., Harrison K. W. and Ha S., *Journal of Applied Physics*, **117** (2015) 112802.

[2] Dingle R., *Physical Review Letters*, **23** (1969) 579.

[3] Garces N. Y., Wang L., Bai L., Giles N. C., Halliburton L. E. and Cantwell G., *Applied Physics Letters*, **81** (2002) 622.

[4] Janotti A. and Van de Walle C. G., *Physical Review B*, **76** (2007) 165202.

[5] Wu X. L., Siu G. G., Fu C. L. and Ong H. C., *Applied Physics Letters*, **78** (2001) 2285.

[6] Vanheusden K., Seager C. H., Warren W. L., Tallant D. R. and Voigt J. A., *Applied Physics Letters*, **68** (1996) 403.

[7] Jie J., Wang G., Han X., Yu Q., Liao Y., Li G. and Hou J., *Chemical Physics Letters*, **387** (2004) 466 .

[8] Liu C., He H., Sun L., Yang Q., Ye Z. and Chen L., *Journal of Applied Physics*, **109** (2011) 053507.

[9] Zhao Q. X., Klason P., Willander M., Zhong H. M., Lu W. and Yang J. H., *Applied Physics Letters*, **87** (2005) 211912.

[10] Stavale F., Pascua L., Nilius N. and Freund H.-J., *The Journal of Physical Chemistry C*, **118** (2014) 13693.

[11] Garces N. Y., Giles N. C., Halliburton L. E., Cantwell G., Eason D. B., Reynolds D. C. and Look D. C., *Applied Physics Letters*, **80** (2002) 1334.

[12] Wang P., He J., Guo L., Yang Y. and Zheng S., *Materials Science in Semiconductor Processing*, **36** (2015) 36 .

[13] Wang X. J., Vlasenko L. S., Pearton S. J., Chen W. M. and Buyanova I. A., *Journal of Physics D: Applied Physics*, **42** (2009) 175411.

[14] Thandavan T. M. K., Gani S. M. A., San Wong C. and Md. Nor R., *PLOS ONE*, **10** (2015) 1.

[15] Chen Y., Zheng C., Ning J., Wang R., Ling C. and Xu S., *Superlattices and Microstructures*, **99** (2016) 208 .

[16] Rodnyi P. A., Chernenko K. A., Zolotarjovs A., Grigorjeva L., Gorokhova E. I. and Venevtsev I. D., *Physics of the Solid State*, **58** (2016) 2055.

[17] Urgessa Z., Mbulanga C., Djiokap S. T., Botha J., Duvenhage M. and Swart H., *Physica B: Condensed Matter*, **480** (2016) 48 .

[18] Dejene F., Onani M., Koao L., Wako A., Motloung S. and Yihunie M., *Physica B: Condensed Matter*, **480** (2016) 63 .

[19] Chen G. Z., Yin J. G., Zhang L. H., Zhang P. X., Wang X. Y., Liu Y. C., Zhang C. L., Gu S. L. and Hang Y., *Crystallography Reports*, **60** (2015) 1147.

[20] Yu J., Lai Y., Cheng S., Zheng Q. and Chen Y., *Journal of Luminescence*, **161** (2015) 330 .

[21] Zhang D. H., Xue Z. Y. and Wang Q. P., *Journal of Physics D: Applied Physics*, **35** (2002) 2837.

[22] Zeng H., Duan G., Li Y., Yang S., Xu X. and Cai W., *Advanced Functional Materials*, **20** (2010) 561.

[23] Han L.-L., Cui L., Wang W.-H., Wang J.-L. and Du X.-W., *Semiconductor Science and Technology*, **27** (2012) 065020.

[24] Vanheusden K., Seager C. H., Warren W. L., Tallant D. R. and Voigt J. A., *Applied Physics Letters*, **68** (1996) 403.

[25] Cao B., Cai W. and Zeng H., *Applied Physics Letters*, **88** (2006) 161101.

[26] Ahn C. H., Kim Y. Y., Kim D. C., Mohanta S. K. and Cho H. K., *Journal of Applied Physics*, **105** (2009) 013502.

[27] Manzano C. V., Alegre D., Caballero-Calero O., Aln B. and Martn-Gonzlez M. S., *Journal of Applied Physics*, **110** (2011) 043538.

[28] Mousavi S., Haratizadeh H. and Minaee H., *Optics Communications*, **284** (2011) 3558 .

[29] Chew Z. J., Brown R. A., Maffeis T. G. and Li L., *Materials Letters*, **72** (2012) 60 .

[30] Mohr P. J., Taylor B. N. and Newell D. B., *Review of Modern Physics*, **84** (2012) 1527.

[31] Levi A. F. J., *Applied Quantum Mechanics* (Cambridge University Press, Cambridge, UK) 2006.

[32] Mooradian A., *Physical Review Letters*, **22** (1969) 185.

[33] Calzolari A. and Nardelli M. B., *Scientific Reports*, **3** (2013) 2999.